MICRO-ARC OXIDATION ENHANCES MECHANICAL PROPERTIES AND CORROSION RESISTANCE OF TI-6AL-7NB ALLOY

Qabas Khalid Naji

Biomedical Engineering Department, AL-Mustaqbal University Collage, Babil, Iraq.

qabas.khalid@mustaqbal-college.edu.iq

Jassim Mohammed Salman

Department of Metallurgical Engineering, College of Materials Engineering, University of Babylon, Iraq.

mat.jassim.mohammed@uobabylon.edu.iq

Nawal Mohammed Dawood

Department of Metallurgical Engineering, College of Materials Engineering, University of Babylon, Iraq.

nawalmohammed2018@gmail.com

Reception: 19/01/2022 **Acceptance**: 07/01/2023 **Publication**: 02/02/2023

Suggested citation:

K. N., Qabas, M. S., Jassim and M. D., Nawal. (2023). **Micro-Arc Oxidation Enhances Mechanical Properties and Corrosion Resistance Of Ti-6Al-7Nb Alloy.** *3C Tecnología. Glosas de innovación aplicada a la pyme, 12(1)*, 262-280. https://doi.org/10.17993/3ctecno.2023.v12n1e43.262-280

ABSTRACT

Investigation results of micro-arc coating on the (Ti-7Nb-6Al) alloy were presented. It has potential clinical value in applications such as dental implant, knee, and hip prostheses. An electrolyte solution of (Na_2CO_3 + Na_2SiO_3). The micro-arc oxidation (MAO) technique was employed for in situ oxidation of Ti-6Al-7Nb surface. The wettability of a porous TiO_2 covering made up of anatase and rutile phases was investigated. The test findings revealed that the possibility of deposition of ceramics coatings on the surface of Ti-6Al-7Nb alloy by using voltages (400V)at different deposition times (7, 15, and 30) min. The results indicate that ceramics layer of titanium oxide (TiO_2) which is formed during coating porous and homogenous distribution. The bioactive composition of the oxide layers can be suitable for use as advanced biomedical implants. The coatings also revealed an increased surface roughness, porosity, microhardness, surface wettability and corrosion resistance of the Ti-6Al-7Nb substrate reaches to (C_R= 0.1114×10^{-3}mpy) in Ringer's solution and (CR= 1.03×10^{-3}mpy) in Saliva's solution with increased deposition time.

KEYWORDS

MAO; Contact Angle; Clinical Application; Oxidation Time; porosity; and Corrosion Resistance

PAPER INDEX

https://doi.org/10.17993/3ctecno.2023.v12n1e43.262-280

1. INTRODUCTION

Metallic are the most important technical materials, and because of their great heat conductivity and mechanical properties, they are used as biomaterials [1]. The most important characteristic of a metal as a biomaterial is that it does not cause an adverse reaction when used in service, which is known as biocompatibility [2]. For load-bearing implants and inner fixing systems, metallic materials are the most frequently used. The primary functions of orthopedic implants systems are to restore the load-bearing joints function that undergo to elevate levels of mechanical stress, wear, and fatigue during ordinary activity [3]. Important orthopedic implants are prostheses for ankle, knee, hip, shoulder, elbow joints and also need equipment like cables, screws, plates, pins, etc. that used in the fixation of fracture [4]. Metals are powerful, and most of them are capable to be formed into complicated forms. During or after final formation, the required mechanical characteristics of metals can be accomplished by heat and mechanical processing. In addition, the correct treatment of components produced from chosen metal compositions can achieve a degree of corrosion and wear resistance. The high tensile strength, high yield strength, fatigue resistance and corrosion resistance are some of the features of metallic materials [5]. In medicine, titanium and its alloys have specific advantages over steels, such as low weight, high corrosion resistance, and a wide range of applications,, low density, low thermal conductivity, non-magnetism, processing workability, and other properties that make it a highly appealing material [6]. Because the modulus of elasticity of titanium and its alloys is closer to that of bone than that of stainless steels and cobalt-based alloys, stress shielding is less of a problem [7]. Because of a TiO2 solid oxide layer, Ti alloys are one of the most common choices in biomedical applications due to their main characteristics. On the other hand, have poor tribological characteristics due to their low resistance to plastic shearing, low work hardening, and lack of surface oxide protection [2]. This titanium surface oxide layer, which is generally a few nanometres thick, has high passivity and resistance to chemical attack [8]. Due to the coarse microstructure of cast alloys (as seen by a high coefficient of friction), weak shear strength, low fatigue strength, and restricted elongation compared to wrought alloys, titanium and its alloys have a high price tag as well as a significant sensitivity to friction and wear. As a result, extra microstructural modification is often required to improve mechanical qualities while maintaining the product's form [9]. The surface of biomedical implants is frequently modified to increase corrosion resistance, wear resistance, surface roughness, and biocompatibility [10]. In addition to increasing other desirable features, all revised surfaces should be evaluated for corrosion behavior. In order to get implants that can survive in the human system for longer periods of time, a thorough understanding of the interactions that occur at the atomic level between the surface of the implant, the host, and the biological environment, as well as all types of micromotions of the implants retained inside the human system, should be researched further [11]. The material surface has a significant impact on the biological environment's response to artificial medical devices [12]. Surface modification does more than simply change the appearance of the surface; it also enhances adhesion properties, micro cleaning, functionalization of amine, and biocompatibility [13]. Many types of surfaces may be created using the surface

https://doi.org/10.17993/3ctecno.2023.v12n1e43.262-280

modification approach to control correct biological response in a specific cell/tissue scenario, with the goal of reducing healing time and limiting harmful reactions [14]. Because titanium and its alloys have poor tribological qualities, such as low wear resistance, they aren't recommended for use in vehicles, the implant's service life is shortened. Surface coatings can help to solve this problem to a considerable extent. Surface engineering can significantly improve the performance of titanium orthopedic devices, allowing them to outperform their inherent capabilities [15]. examples of surface modification processes: physical and chemical method, laser cladding, thermal oxidation, plasma spray, and ion implantation [16].

2. MATERIALS AND METHODS

In the test, Ti-6Al-7Nb alloy with element composition of 6.3Al, 67Nb, 0.47Ta, 0.23Fe, 0.18O, 0.077C, 0.046N,0.0088H, and the balance Ti (wt%) were used as raw materials. The substrate was sliced into 13 mm x 3 mm round wafers and polished using SiC abrasive sheets ranging from 150 to 5000 grit. After that, ultrasonic cleaning with acetone, alcohol, and deionized water was performed. The ceramic coatings were deposited using a DC-AC homemade MAO deposition device with a voltage of (0-500) V and a current of (0-5) A MAO with an impulse frequency of 500 Hz, current density of 20 A/cm2, duty cycle of 10%, and oxidation durations of 7 minutes, 15 minutes, and 30 minutes at voltage 400V. Deionized water and 10 g/L sodium carbonite and 2 g/L sodium silicate were used to make the electrolyte solution. Following the ultrasonic processing of the MAO test sample, the sample was dried and set aside.

3. RESULTS AND DISCUSSION

3.1. CHARACTERIZATION OF OXIDE SURFACE

In Fig.1 (a) The XRD results proved the deposition of titanium oxide layer after MAO on the surface of the Ti-6Al-7Nb alloy substrate at 7min. The formation of TiO2 layer on the surface of specimen A3 has crystalline phases: rutile (tetragonal) and anatase (tetragonal) phases also the (α-HCP) and (β-BCC) return to the Ti-alloy. The peaks of rutile TiO2 (200), (211), and (202) at 2Θ° (39.3, 54.2, and 76.0) and those of titania crystals structures (anatase) (101), (103), and (200) at 2Θ° (25.9, 37.9, and 48.3) strength of the Ti-6Al-7Nb alloy peaks reduced compared to the untreated Ti sample. This is due to the crystal structure of both types, the energy gaps for anatase are more than those of rutile, this makes the anatase more pores and it’s used in optical application while the rutile is with low energy gape and more stable at high temperatures and more important for medical application [17]. Limiting voltage increased, perhaps due to oxide layer formation as illustrated in Fig.1 (b) at 15min. For the highest deposition time in Fig.1 (c). the presence of anatase indicates that throughout the MAO process, a significant oxidation reaction took place on a titanium surface. As a result, the combination of anatase and rutile crystal phases in the coated

https://doi.org/10.17993/3ctecno.2023.v12n1e43.262-280

Ti-alloys specimen developed in this work is expected to have a positive influence on Ti-alloy bioactivity by enhancing their osteogenic properties. It is also suggests that predominantly anatase is created at lower forming voltages, however because anatase, as a metastable phase, gradually converts into rutile at higher temperatures as dielectric breakdown processes increase, the mixture of anatase and rutile phases develops at increased deposition time [18].

(a)

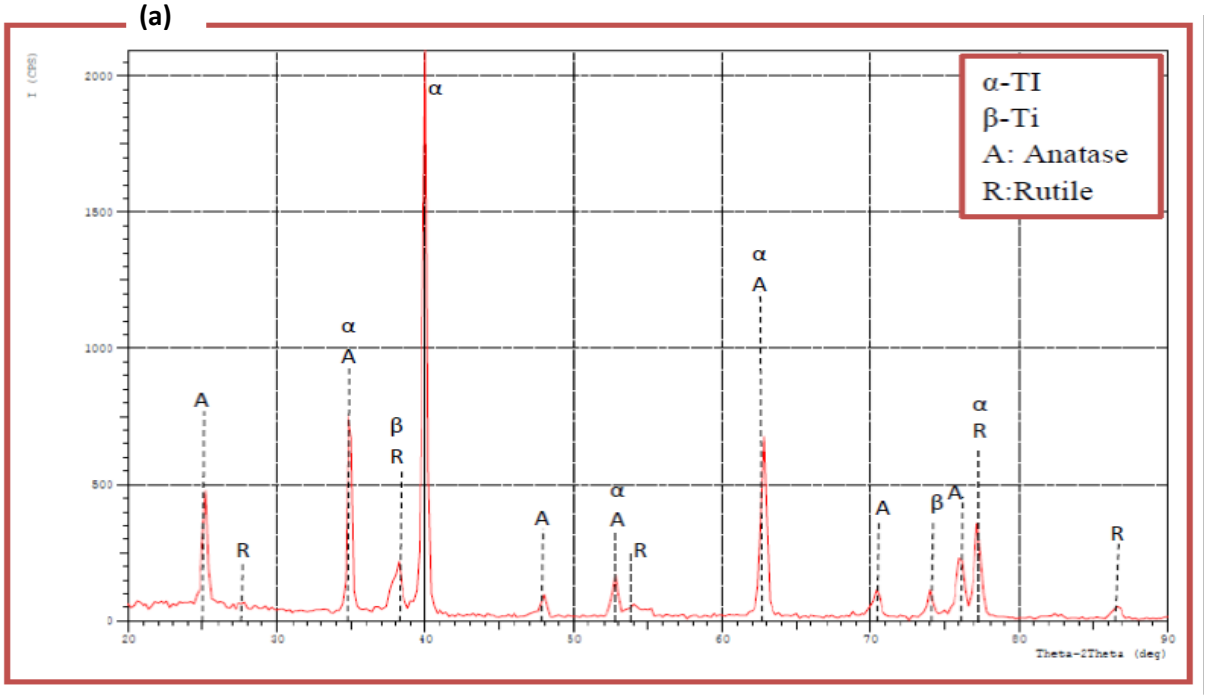

(b)

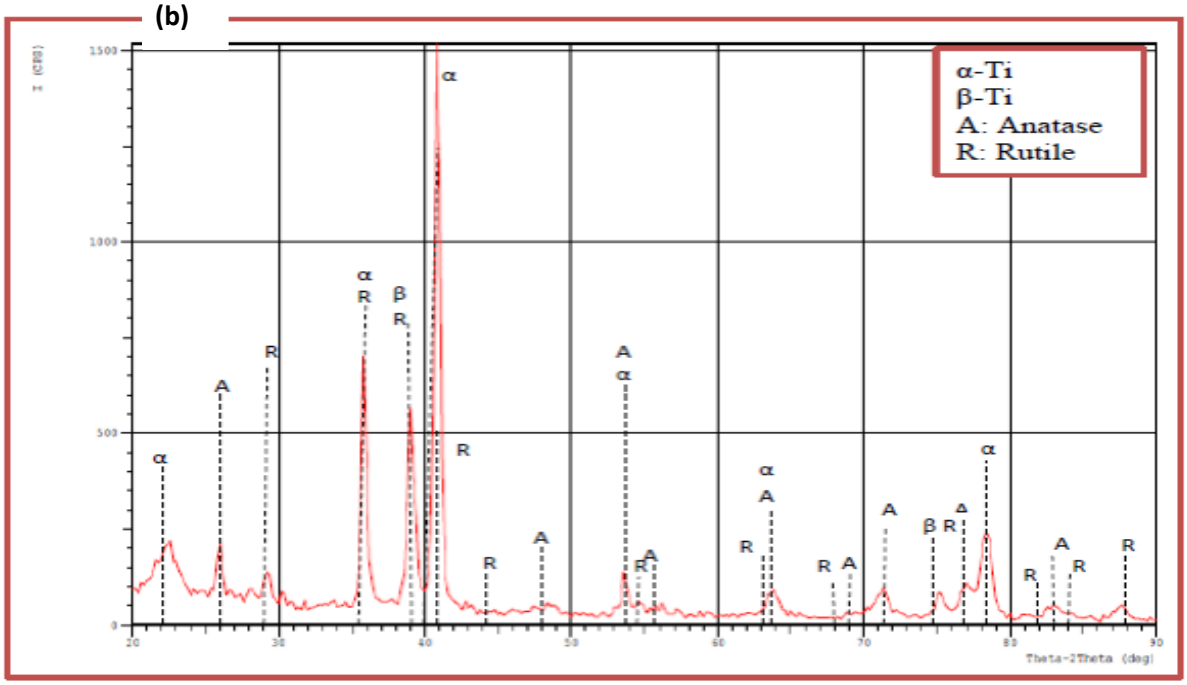

(c)

https://doi.org/10.17993/3ctecno.2023.v12n1e43.262-280

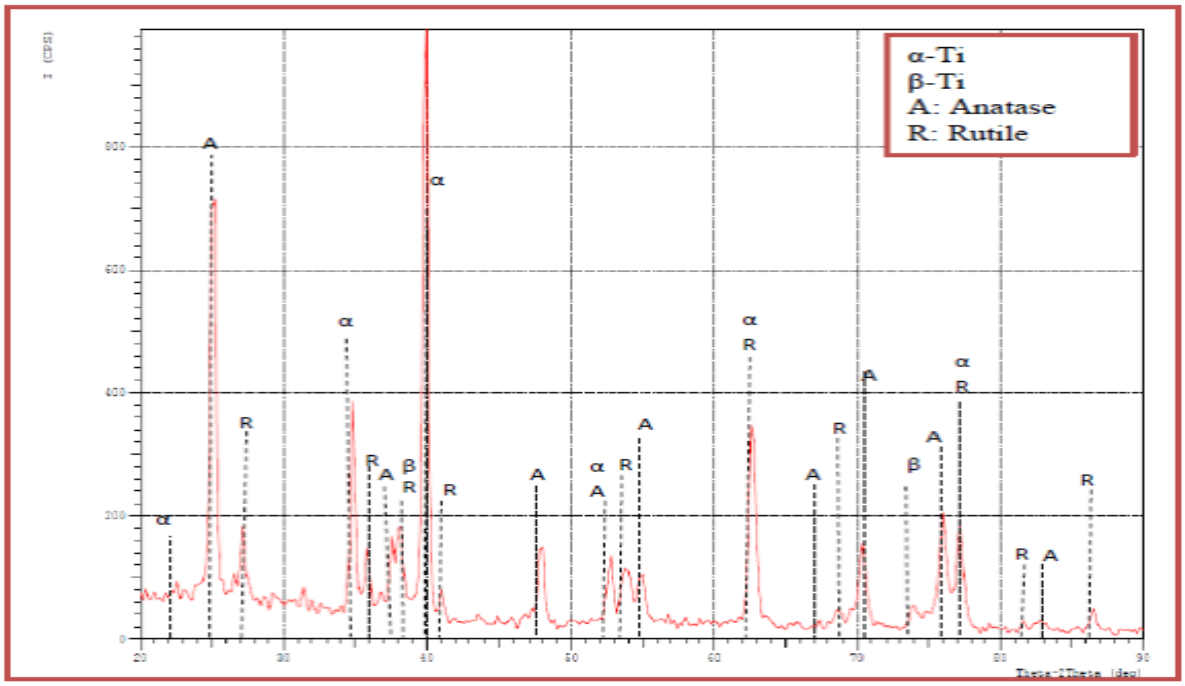

Figure 1. XRD of MAO Process with different time (a) coating at 7min, (c) coating at 15min, and (d) coating at 30min.

The FESEM results of microstructure coated specimen from Fig.2 which show that for surface morphology of the oxide layer TiO2 to the Ti-6Al-7Nb alloys at different magnifications treated by MAO process relatively rougher and exhibited a grainy structure with limited amount of pores with different sizes by the spark discharges. Micro-pores and submicron-pores were visible in the MAO coating, with the micro-pores having a roughly round or elliptical form like a volcanic vent [19].

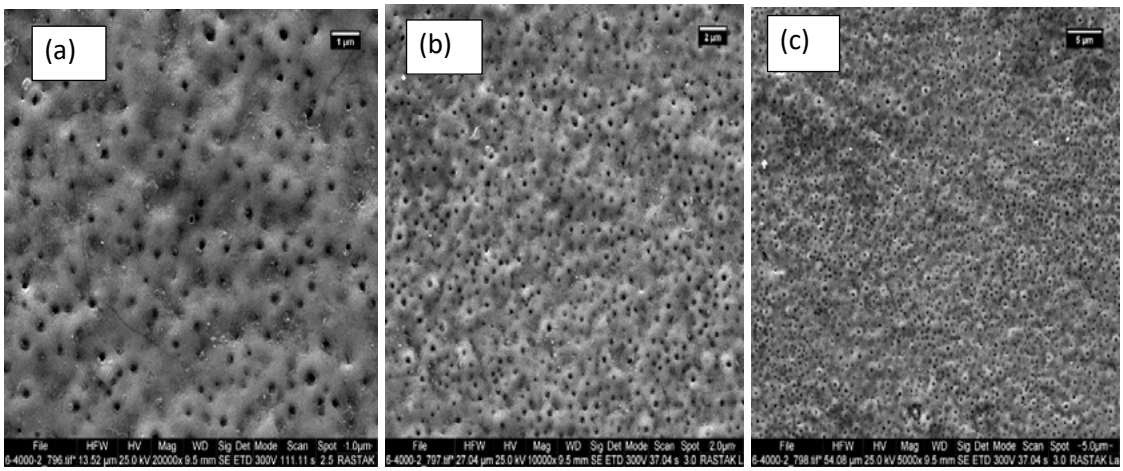

https://doi.org/10.17993/3ctecno.2023.v12n1e43.262-280

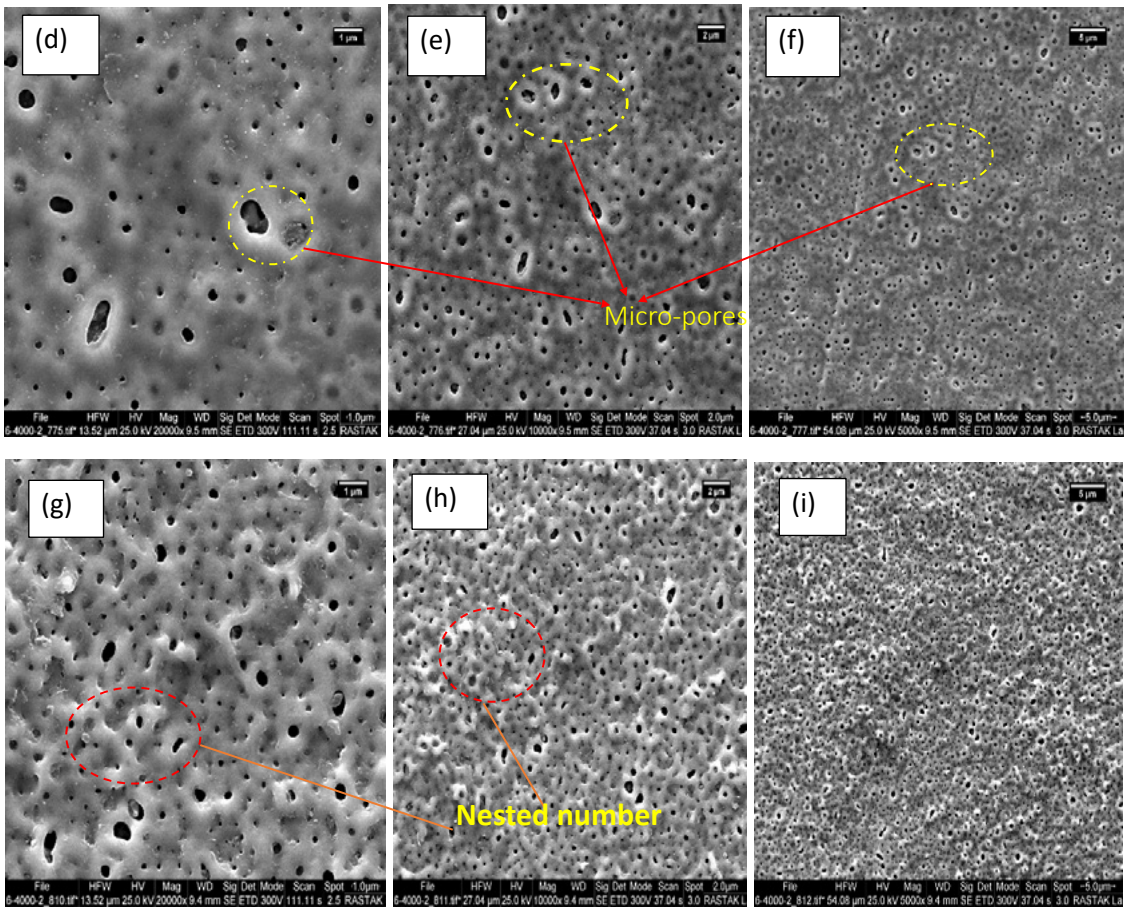

Figure 2. FESEM Micrographs of TiO2 coating MAO process at different magnification and time.

A typical porous structure was also found in coating of sample at 15min. Pores with miximum diameters and homogenous distribution can be observed on the surface of the Ti-alloy. The diameters of the such holes and the surface roughness grew as the voltage rose; after 30 min of treatment, the pores diameters increased, and the coated surface progressively became rough. The oxide layer on both materials is formed by several micro-protrusions with uniformly scattered pores with diameters varying from sub-micron to few microns. When compared to a polished surface that hasn't been covered, the presence of this porosity improves osseointegration because the pores function as sites for bone tissue formation, hence improving anchoring [20]. The FESEM cross-sectional morphology of TiO2 coating layer has a regular thin film structure in thickness with more compact, homogeneity, and full adhesion between the coating and the underlying substrate, as shown in Fig. 3 (a). each sample's coating layer has a compact diffusion layer in contact with the substrate and an external porous conversion zone with discharge channels make up the two sections. The average thickness of the diffusion layer remains constant throughout the procedure. the average thickness of the external porous conversion layer rises as the deposition duration increased, from 1.94μm at 7 min to 5.54μm at 30 min, as shown in Fig.3 (b and c).

https://doi.org/10.17993/3ctecno.2023.v12n1e43.262-280

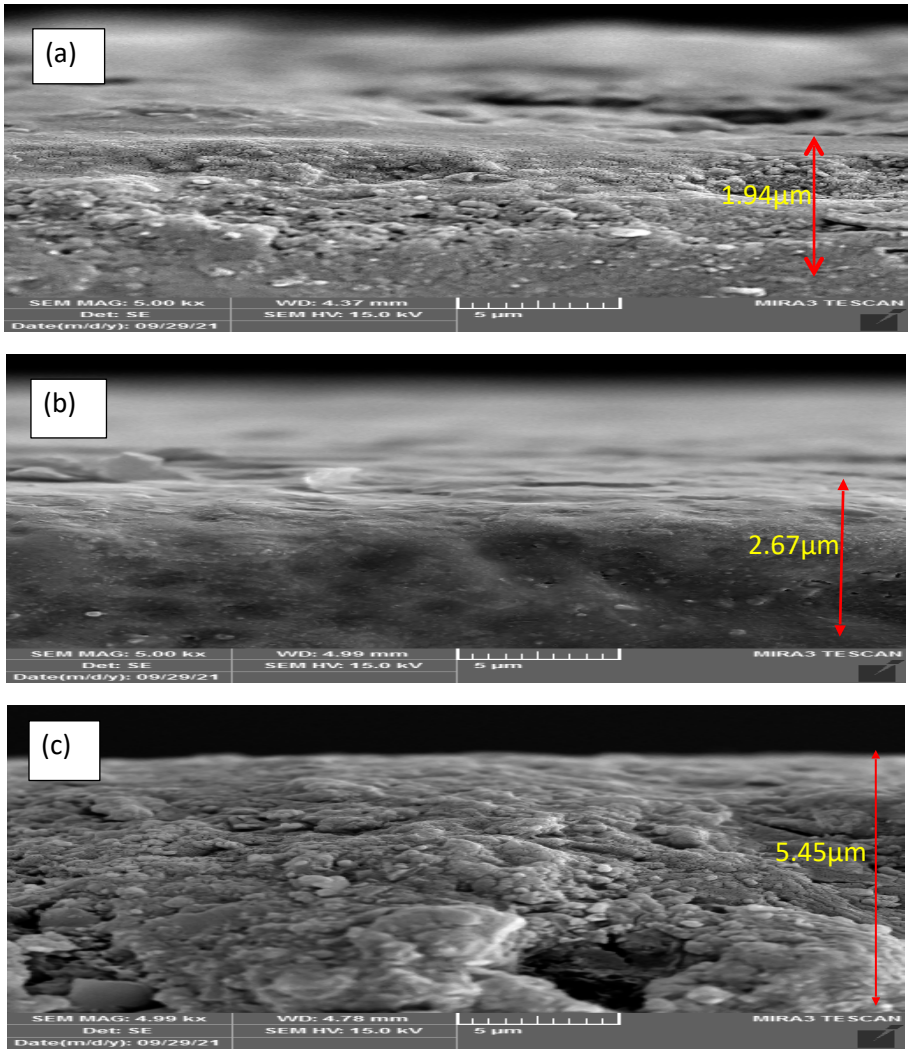

Figure 3. Cross section of MAO coatings: (a) at 7min, (b) 15min, and (c) 30min.

The formation of crossing pores and big pores distributed along the whole thickness. Generally, the coating thickness is increased with increasing deposition time because the voltage on the sample could not reach the sparking threshold, and a thin layer of oxide film quickly formed on the sample surface because of anodic oxidation. When the oxidation time was increased, the sparking voltage was reached and the energy rose; consequently, some discharge channels on the specimens became evident. Oxide film formed on the inner and outer surfaces of the discharge channel as the reaction product erupted along the channel. The oxide coating thickened when the oxidation duration, and energy were increased. Furthermore, the molten oxide spilled over the discharge tube, immediately cooled, and was deposited on the surface. The process was repeated until the end of the oxidation reaction, causing incessant growth of the oxide film [21]. The Presents of schematic data of EDS results for MAO TiO2 coatings with different times on containing Ti, O, Al, and Nb ions. EDS analysis showed that increasing of time up to 30 min had it effects on the content of oxide layer as shown in Fig.4 coated with different times. As a result of the presence of Ti and O2 components in the coatings, TiO2 layers with varied weights of these modification elements.

https://doi.org/10.17993/3ctecno.2023.v12n1e43.262-280

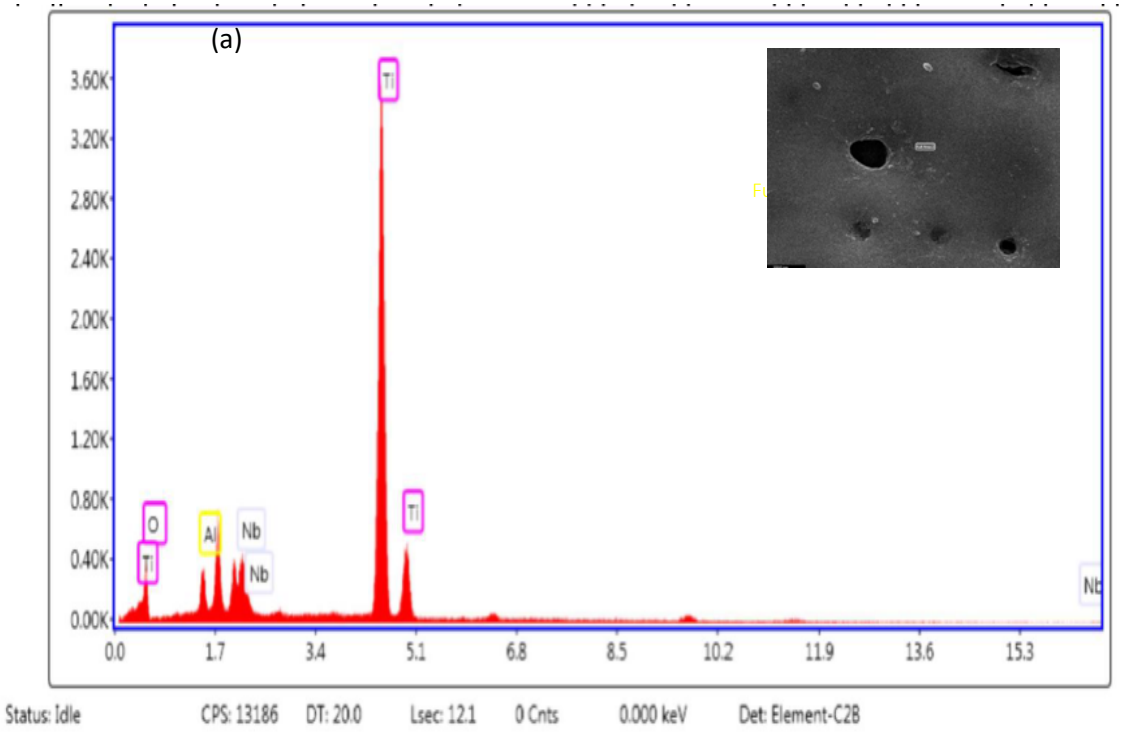

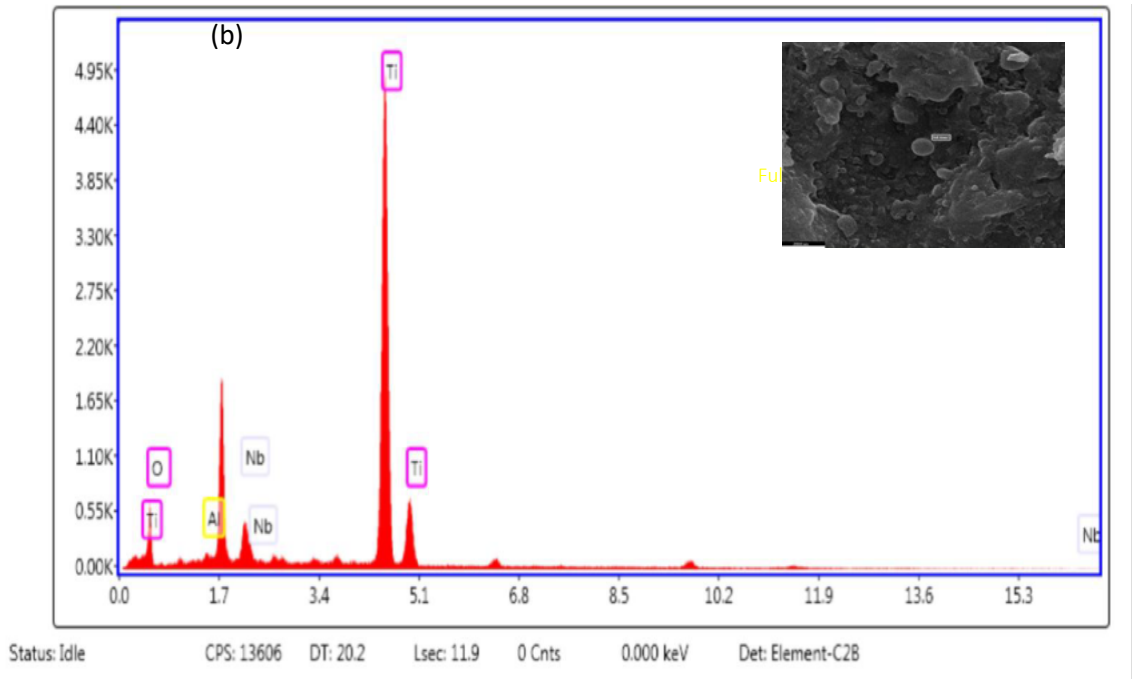

https://doi.org/10.17993/3ctecno.2023.v12n1e43.262-280

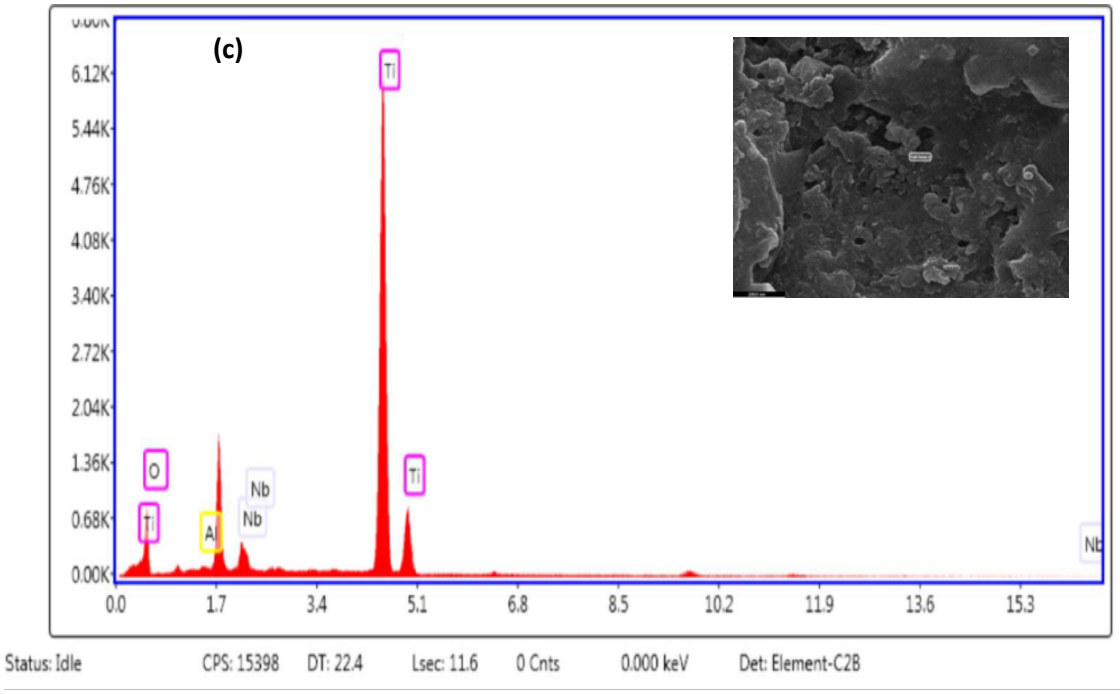

Figure 4. EDS result of (a) coating at 7min, (b) coating at 15min, and (c) coating at 30min.

Results of AFM analysis are given in Fig.5, the differences in surface topography between the substrate and different coatings in 2D and 3D, where observed an increase in the roughness of the TiO2 coatings because of the phenomena of micro-discharge resulting from the nature of the MAO process [22]. The Ra of coatings were more than those of the substrates and increased with time roughness also increased from (7.19nm) for 7min, (12.6nm) for 15min, and (18.8nm) for 30min because increase oxidation time.

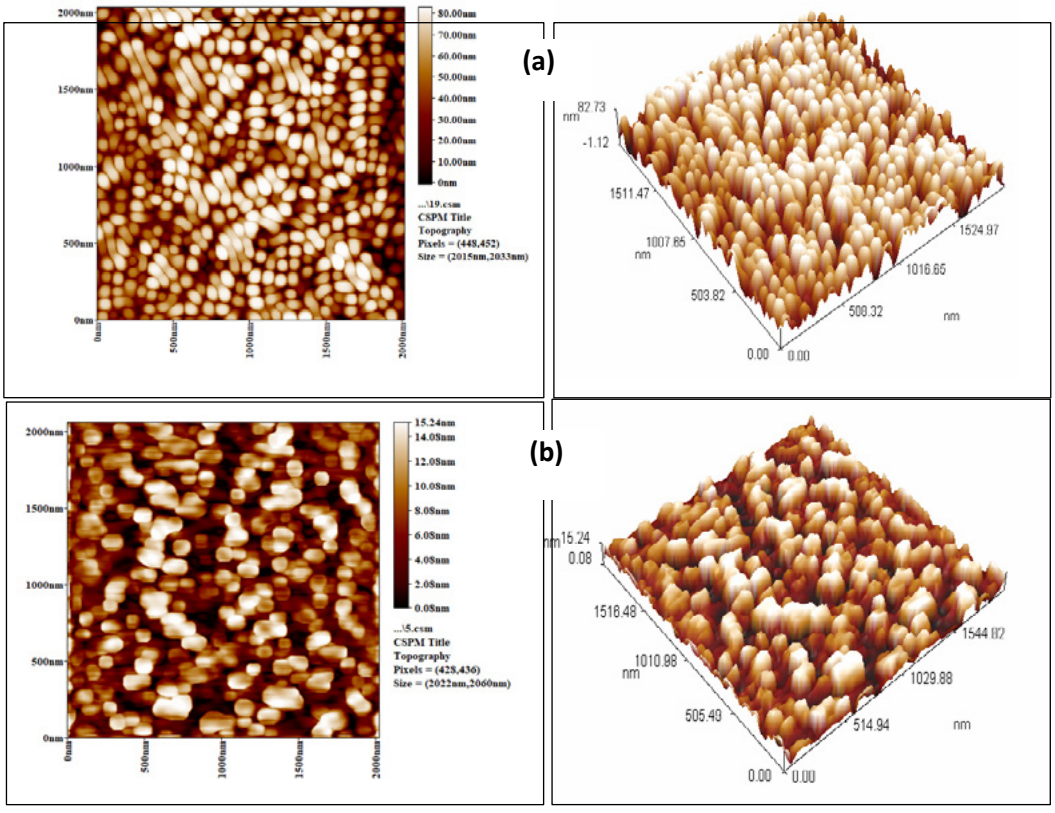

https://doi.org/10.17993/3ctecno.2023.v12n1e43.262-280

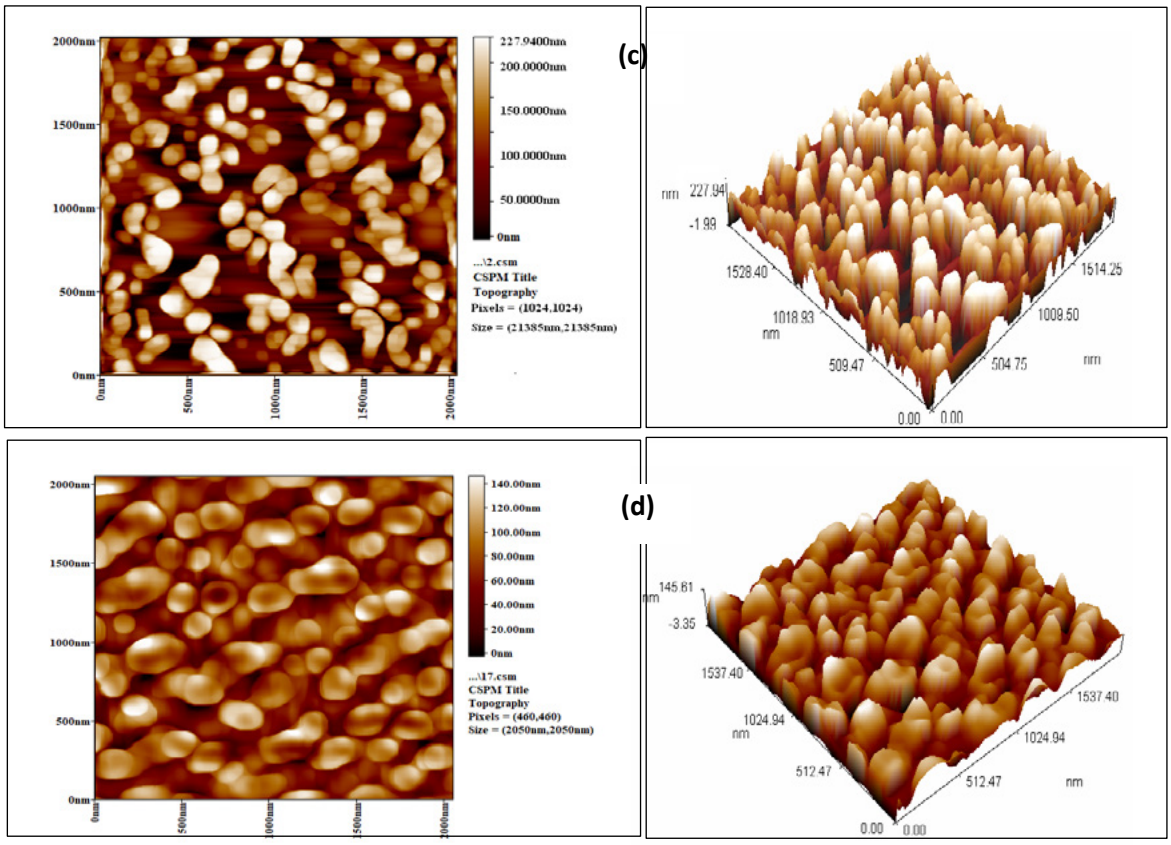

Figure 5. AFM results of samples (a) base, (b) coating at 7min, (c) coating 15min, and (d) coating 30min.

3.2. MECHANICAL PROPERTIES:

Results of micro-hardness at TiO2 of the coated samples at a load of 50gm (0.49N) using a fixed loading duration of (15sec.) in Fig.6. In general, it can be observed that the hardness of coated samples is improved by MAO process. The value of hardness equal to (268.55 HV at 7min) are significantly higher than that of Ti-6Al-7Nb alloy, and the increase hardness value with increase the deposition time to the (311.5 at 15min) because the production of dense oxide layer, which is attributed to formation of thermal micro arcs during MAO and increase thickness of ceramic coating [17]. The MAO treated sample's greater standard deviations might also be attributed to their higher surface porosity. Which resulted in lower leading hardness at the interface (287.3HV at 30min).

https://doi.org/10.17993/3ctecno.2023.v12n1e43.262-280

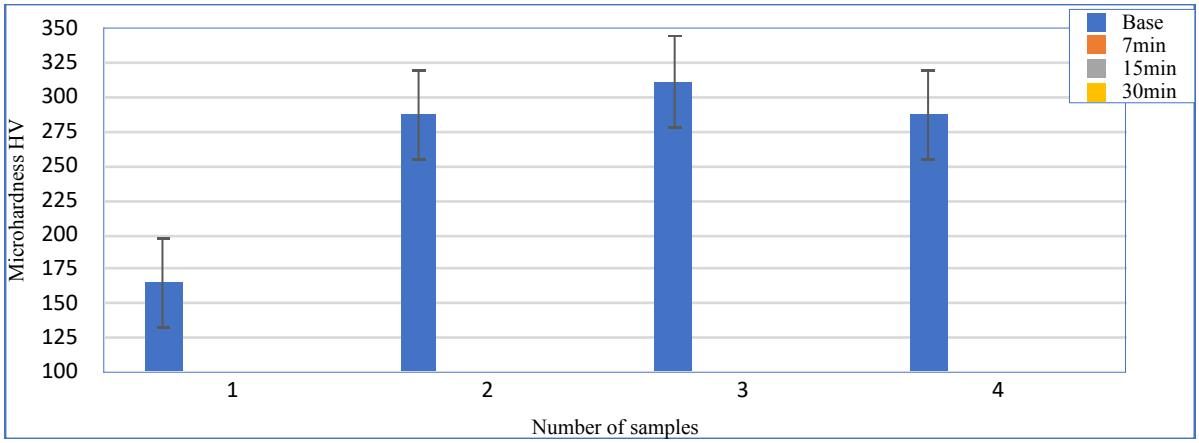

Figure 6. Relationship between the deposition time and the micro-hardness of coatings at TiO2 by MAO process.

Wear resistance is one of the most significant implant mechanical properties that wear failure contributes from all implant's failure reasons. Wear mass loss of test specimens under 10N stress and several times (5, 10, 15, 20, 25, and 30) min were used to evaluate the wear rates produced by pin-on disc sliding wear tests. Generally, it can be observed that the weight loss increased with increasing of loading time. Fig.7 shows that high wear rate of Ti-6Al-7Nb alloy substrate comparison, with coating. The ceramic oxide layers were found to have high wear resistance, resulting in a lower wear rate in the samples. ceramic coatings deposited TiO2 by MAO process, gave the best wear resistance and low wear rate $\left(2.78 \times 10^{-5}\right)$ at 7min. Due to improved hardness by presence of the alpha and beta titanium phases and presence of modified elements could be reduce the friction and increase wear resistance of coating by reduce wear rate. The intensity of micro-discharges rises as the applied duration increases (30min), resulting in an increase in coating porosity owing to a decrease in coating electric resistance. The coating porosity distribution has an impact on both mechanical and tribological properties [23]. This is supported by the current findings, which reveal that the coating has greater wear rates equal $\left(9.46 \times 10^{-6}\right)$ after passing 30min.

https://doi.org/10.17993/3ctecno.2023.v12n1e43.262-280

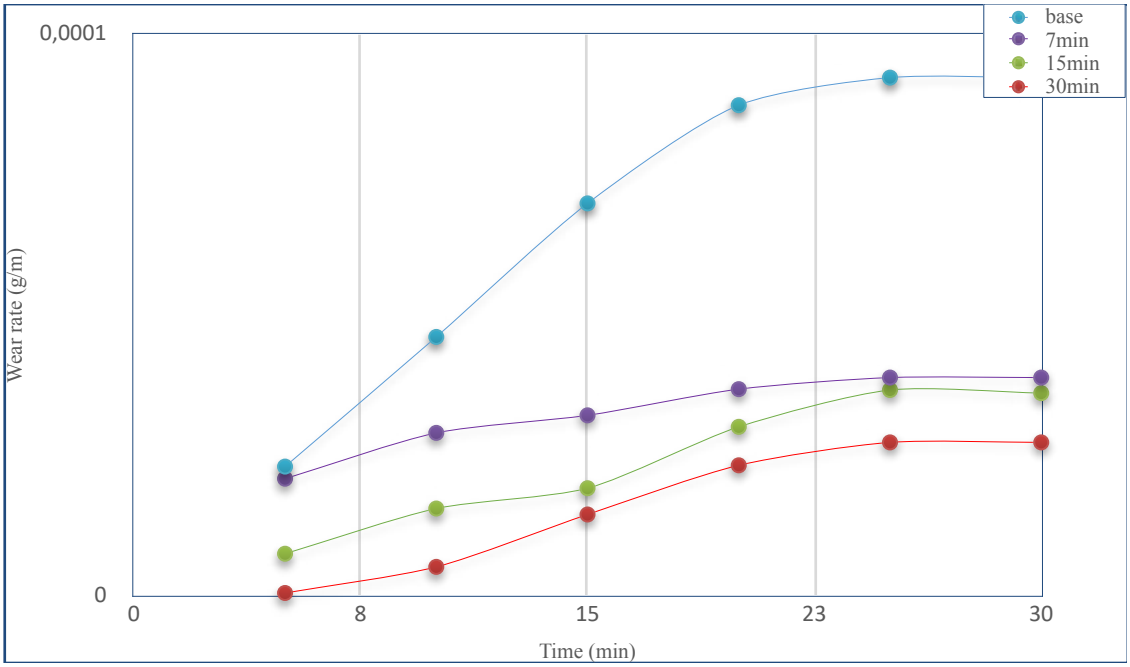

Figure 7. Relationship between wear rate and test time for Ti-6Al-7Nb alloy substrate and MAO process with different deposition time.

3.3. CONTACT ANGLE TEST

The contact angle, which is an essential measuring tool for determining material surface wettability was also discovered to be a key factor in increasing the bioactivity of titanium surfaces. Fig.8 show the contact angles tested of TiO2 by MAO coatings prepared at various deposition times in Ringer's and Saliva's solution. With increased surface roughness and porosity, the specimen's contact angle reduces considerably following MAO treatment. The contact angle reached value to (56.74° at 7min in ringer's solution and 54.7° in saliva's solution) and decreased with increase deposition time reached to (11° at 30min in ringer solution and 13.1° in saliva solution). The MAO treatment resulted in an uneven coating surface, increased roughness, increased absorbability, and decreased contact angles, all of which together affected the surface energy; and the OH and O2 oxygen-containing groups produced on the coated surfboard. These factors combined to increase the wettability of the MAO treated because a large number of micro/nano-pores formed on the oxidation coating surface caused its specific surface area to oxidation coating increase, which benefited water retention [24].

https://doi.org/10.17993/3ctecno.2023.v12n1e43.262-280

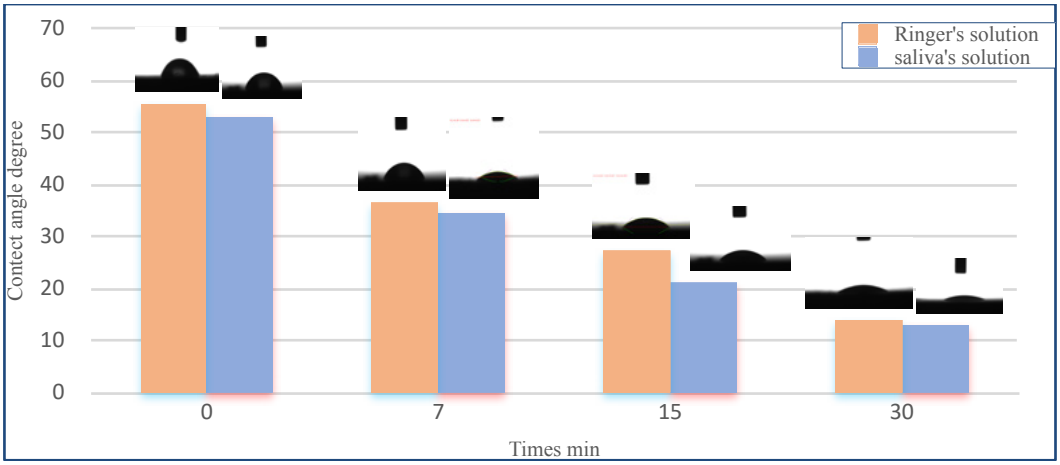

Figure 8. Results of contact angle in TiO2 at 400V in Ringer's and Saliva's solution.

3.4. ELECTROCHEMICAL BEHAVIOR OF THE ALLOY/OXIDE SYSTEMS

The potentiodynamic polarization curves for the Ti-6Al-7Nb alloy substrate and TiO2 coated by MAO process samples in Ringer's solution at 37°C±1 at various times in Fig. 9. Tafel extrapolation is used to calculate the corrosion current densities (icorr.) and corrosion potentials (Ecorr.) using potentiodynamic curves, and corrosion rates (CR) were also included in Table.1. It can be seen from the results obtained in the uncoated substrate has a greater corrosion current density (icorr= 6.8284 A/cm2) of thus lowest corrosion resistance because of the occurrence of metal ions dissolution on the surface of the uncoated substrate. The corrosion current density and corrosion rate of all coated samples by MAO decrease after TiO2 coating, indicating that the TiO2 coating offers a protective layer on the substrate surface that reduces corrosion rate. The lowest corrosion current (icorr. = 2.8161 A/cm2) and increased corrosion potential of the specimens are achieved when coating for 7 min, and this result has a reduced corrosion rate equal to (CR= 3.48×10-3 mpy), indicating that corrosion resistance is improved. Furthermore, the film's surface structure influences the material's corrosive qualities. Materials with denser and thicker oxide layers have a lower corrosion current density and a lower corrosion rate (icorr. = 0.0902A/cm2), and a lower corrosion rate (CR=0.111×10-3 mpy) at (15min).

https://doi.org/10.17993/3ctecno.2023.v12n1e43.262-280

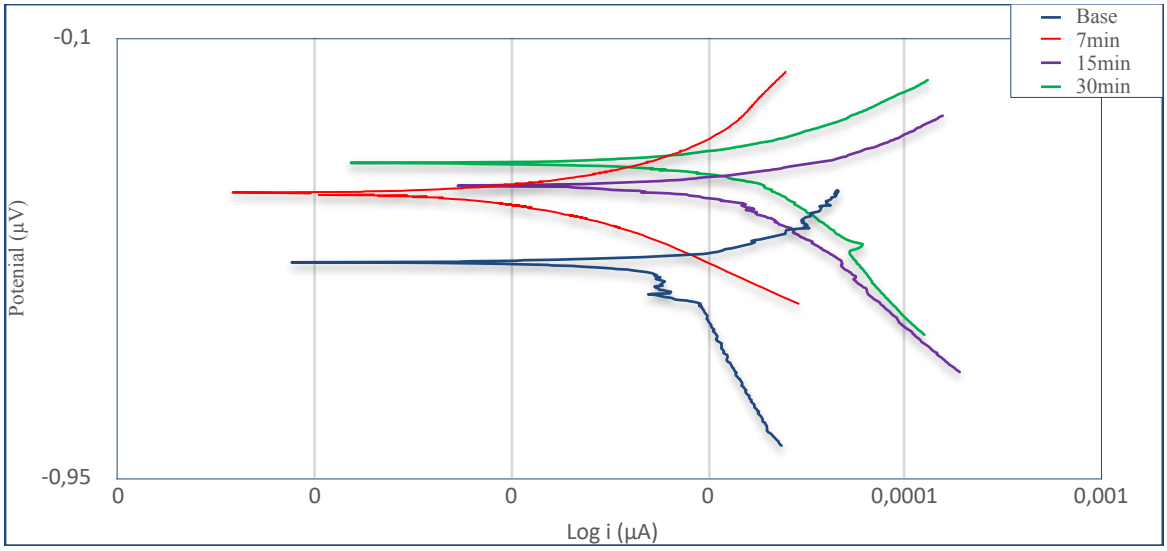

Figure 9. Potentiodynamic polarization curves of TiO2 coated by MAO process and base at different time in Ringer's solution.

The porosity affected the corrosion behavior of highly porous where decreased corrosion resistance because increased (icorr. =1.3643 µA/cm2) and (CR =1.686×10-3mpy). The corrosion behavior of porous metallic materials has in the present work, the oxygen/air entrapped in the most inner pores neither the difficulty of electrolyte penetration into these pores, may result in various passive states on the native oxide surface. The surface area, on the other hand, has minimal influence on the corrosion rate of porous materials. Although Ti is known for its strong resistance to localized corrosion, and localized breakdown of its passive coating occurs at substantially higher potentials, the increased corrosion density with greater porosity level is due to the larger surface area in contact with the electrolyte, but fissures or restrictions to the flow of species into the connected pores can result in corrosion rates that are not proportional to the real contact surface area. Although these challenges may result in faster corrosion rates, good passivation qualities for porous Ti structures have been documented in the literature. On the other hand, increased porosity was also associated with a decreased susceptibility to corrosion (less negative Ecorr.), as interconnected pores encouraged the free flow of ionic species, whereas isolated pores trapped the electrolyte and depleted the oxygen supply, leading to a thinner oxide film. Aside from species free movement, air entrapment, and electrolyte penetration [25].

https://doi.org/10.17993/3ctecno.2023.v12n1e43.262-280

Table.1. Electrochemical parameters of base and TiO2 coated MAO at different time in Ringer's solution.

Parameters of coating	$i_{corr.}$ (μA/cm²)	$E_{corr.}$ (mV)	Rate of Corrosion (mpy)×10⁻³	Enhancement percentage (%)
base	6.8284	-533	8.437	/
7min	2.8161	-342	3.480	58.7
15min	0.0902	-341	0.111	98
30min	1.3643	-390	1.686	80

The corrosion behavior in Saliva's solution of the alloy and coated samples TiO2 by MAO process in Fig.10 respectively, and Table.2 it is clear, that the specimen showed relatively similar behavior to that observed in saliva's solution such as MAO process for alloy improved corrosion resistance because of reduction in corrosion current [26,27]].

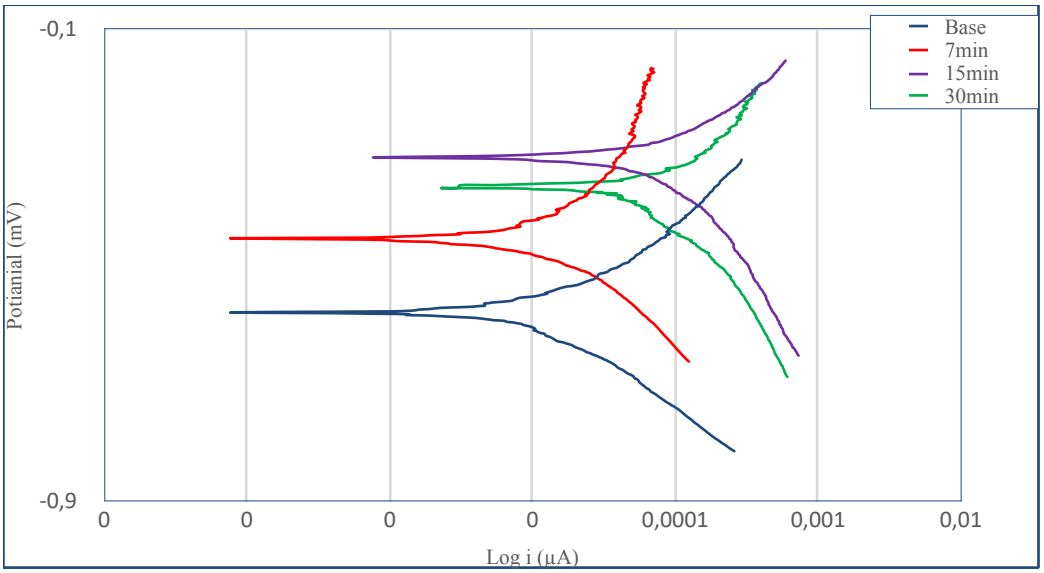

Figure 10. Potentiodynamic polarization curves of TiO2 coating by MAO process and base at different time in Saliva's solution.

Table 2. Electrochemical parameters of base and TiO2 coated MAO at different time in Saliva's solution

Parameters of coating	$i_{corr.}$ (μA/cm²)	$E_{corr.}$ (mV)	Rate of Corrosion (mpy)×10⁻³	Enhancement percentage (%)
base	7.103	-579	8.777	/
7min	3.479	-491	4.3	51
15min	0.833	-472	1.03	88.26
30min	1.475	-392	1.8	79.5

https://doi.org/10.17993/3ctecno.2023.v12n1e43.262-280

4. CONCLUSION

In the current study, the TiO2 coating has been deposited on the surface of Ti-6Al-7Nb alloy successfully by using micro-arc oxidation process for biomedical applications.

1. The TiO2 layer formed on Ti-6Al-7Nb alloy substrate material using MAO methods has circular micro holes in rough and volcanic structures because of continuous micro discharges occurring during the process. Rutile TiO2 and anatase TiO2 phases are determined on the material surface following the XRD analysis.
2. The substrate's surface roughness plays has an important role to improving coating-substrate adhesion. AFM topography shows homogeneous and dense at (30 min).
3. EDS results showed that the ratio of Ti/O increased with time at coating.
4. The apparent contact angle somewhat reduces following treatment at various times. The surface morphology and composition of the MAO coatings may be the cause of the MAO coatings' considerable shift in apparent contact angle. Due to its smaller pores, the wettability of the MAO coating created at lower roughness may be underestimated. It's possible that the wettability of the MAO coating generated at reduced roughness is overestimated. The wettability of the MAO coating generated at higher roughness may be overstated since no gas is trapped and the liquid/solid interface is rougher.
5. The potentiodynamic polarization results that Ti-6Al-7Nb base alloy substrate and TiO2 at different times in Ringer's and Saliva's solutions; the best result equal (icorr.=0.0902μA/cm2) in Ringer's solution and (icorr.= 0.833μA/cm2) in Saliva's solution compared to the uncoated sample.

ACKNOWLEDGEMENTS

The Authors are grateful for the University of Babylon for their help. Special thanks for, AL Mustaqbal University Collage, Biomedical Engineering Department.

REFERENCES

(1) L. Thair, U. K. Mudali, N. Bhuvaneswaran, K. G. M. Nair, R. Asokamani, and B. Raj. (2002). **Nitrogen ion implantation and in vitro corrosion behavior of as-cast Ti-6Al-7Nb alloy.** *Corros. Sci.*, 44(11), 2439-2457.

(2) G. Wu, P. Li, H. Feng, X. Zhang, and P. K. Chu. (2015). **Engineering and functionalization of biomaterials via surface modification.** *J. Mater. Chem. B*, 3(10), 2024-2042.

(3) A. T. Sidambe. (2014). **Biocompatibility of advanced manufactured titanium implants-A review.** *Materials (Basel)*, 7(12), 8168-8188.

(4) M. kawano, Y. Takeda, K.Ogasawara. (2015). **Pathological Analysis of Metal Allergy to Metallic Materials,** 305-321.

https://doi.org/10.17993/3ctecno.2023.v12n1e43.262-280

(5) G. A. dos Santos. (2017). **The Importance of Metallic Materials as Biomaterials.** *Adv. Tissue Eng. Regen. Med. Open Access*, 3(1), 300-302, 2017.

(6) L. Mohan and C. Anandan. (2013). **Wear and corrosion behavior of oxygen implanted biomedical titanium alloy Ti-13Nb-13Zr.** *Appl. Surf. Sci.*, 282, 281-290.

(7) N. Mitsuo. (1998). **Mechanical properties of biomedical titanium alloys.** *Mater. Sci. Eng. A.*, 243(1-2), 231-236.

(8) S. Shaikh, S. Kedia, D. Singh, M. Subramanian, and S. Sinha. (2019). **Surface texturing of Ti6Al4V alloy using femtosecond laser for superior antibacterial performance.** *J. Laser Appl.*, 31(2), 022011.

(9) Y. X. Leng, J. Y. Chen, P. Yang, H. Sun, and N. Huang. (2003). **Structure and properties of passivating titanium oxide films fabricated by DC plasma oxidation**. *Surf. Coatings Technol.*, 166(2-3), 176-182.

(10) M. Almasri. (2016). **Introductory Chapter : Dental Implantology, The Challenging Scenarios between Training, Resources, and Patients' Demands.** *Dent. Implantol. Biomater.*

(11) S. V. Dorozhkin. (2015). **Calcium orthophosphate deposits: Preparation, properties and biomedical applications.** *Mater. Sci. Eng. C*, 55 272-326.

(12) A. Prof and A. Prof. (2019). **Surface modification of titanium and titanium alloys: technologies, developments and future interests,** 10, 12-58.

(13) H. Chouirfa, H. Bouloussa, V. Migonney, and C. Falentin-Daudré. (2019). **Review of titanium surface modification techniques and coatings for antibacterial applications.** *Acta Biomater.*, 83, 37-54.

(14) L. C. Zhang and L. Y. Chen. (2019). **A Review on Biomedical Titanium Alloys: Recent Progress and Prospect.** *Adv. Eng. Mater.*, 21(4), 1-29.

(15) [15] Liu, Xuanyong, Chu, Paul K., and Ding, Chuanxian. (2004). **Surface modification of titanium, titanium alloys, and related materials for biomedical applications.** *Materials Science and Engineering R: Reports*, 47(3-4), 49-121.

(16) M. T. Mohammed, Z. A. Khan, and A. N. Siddiquee. (2014). **Surface Modifications of Titanium Materials for developing Corrosion Behavior in Human Body Environment: A Review.** *Procedia Mater. Sci.*, 6(no. Icmpc), 1610-1618.

(17) A. Santos-Coquillat, R. Gonzalez Tenorio, M. Mohedano, E. Martinez-Campos, R. Arrabal, and E. Matykina. (2018). **Tailoring of antibacterial and osteogenic properties of Ti6Al4V by plasma electrolytic oxidation.** *Appl. Surf. Sci.*, 454, 157-172.

(18) V. S. De Viteri et al. (2016). **Structure, tribocorrosion and biocide characterization of Ca, P and I containing TiO 2 coatings developed by plasma electrolytic oxidation.** *Appl. Surf. Sci.*, 367, 1-10.

(19) L. Xu et al. (2018). **Effect of oxidation time on cytocompatibility of ultrafine-grained pure Ti in micro-arc oxidation treatment.** *Surf. Coatings Technol.*, 342, 12-22.

https://doi.org/10.17993/3ctecno.2023.v12n1e43.262-280

(20) L. C. Campanelli, L. T. Duarte, P. S. C. P. da Silva, and C. Bolfarini. (2014). **Fatigue behavior of modified surface of Ti-6Al-7Nb and CP-Ti by micro-arc oxidation.** *Mater. Des.*, 64, 393-399.

(21) M. Shamsuzzoha, and E.Development. (2014). **TMS2014 Annual Meeting Supplemental Proceedings.** *The Minerals, Metals & Materials Society*, 1, 1057-1062.

(22) D. Quintero et al. (2017). **Anodic films obtained on Ti6Al4V in aluminate solutions by spark anodizing: Effect of OH− and WO4− 2 additions on the tribological properties.** *Surf. Coatings Technol.*, 310, 180-189.

(23) X. Shen, P. Shukla, S. Nath, and J. Lawrence. (2017). **Improvement in mechanical properties of titanium alloy (Ti-6Al-7Nb) subject to multiple laser shock peening.** *Surf. Coatings Technol.*, 327, 101-109.

(24) A. Cunha. (2015). **Multiscale femtosecond laser surface texturing of titanium and titanium alloys for dental and orthopaedic implants**, *University De Bordeaux.*

(25) M. B. Sedelnikova et al. (2020). **Functionalization of pure titanium MAO coatings by surface modifications for biomedical applications.** *Surf. Coatings Technol.*, 394(march), 125812.

(26) A. Khandan, N. Ozada, D. Ogbemudia, and S. Saber-Samandari. (2017). **Novel technology for bone cancer tumor by using hyperthermia treatment via bioceramic mechanism.** *UFGNSM*, 12, 13.

(27) Kumbhalkar, M.A., Rangari, D.T., Pawar, R.D., Phadtare, R.A., Raut, K.R., Nagre, A.N. (2021). **Finite Element Analysis of Knee Joint with Special Emphasis on Patellar Implant**. *Trends in Mechanical and Biomedical Design. Lecture Notes in Mechanical Engineering. Springer*.

https://doi.org/10.17993/3ctecno.2023.v12n1e43.262-280